Supporting Information: Femtosecond Laser Induced Non-Thermal Welding for Single Cu Nanowire Glucose Sensor

Yongchao Yu[1], Yangbao Deng [2], Md Abdullah Al Hasan[1], Yanfeng Bai[1,3] Ruozhou Li[4], Shuguang Deng[2], Pooran Joshi [5], Seungha Shin[1], and Anming Hu[1]**

[1]Department of Mechanical, Aerospace and Biomedical Engineering, University of Tennessee Knoxville, 1512 Middle Drive, Knoxville, TN 37996, USA

[2]All-solid-state Energy Storage Materials and Devices Key Laboratory of Hunan Province, College of Information and Electronic Engineering, Hunan City University, Yiyang 413000, P. R. China

[3]College of Computer Science and Electronic Engineering, Hunan University, Changsha 410082, P. R. China

[4]College of Electronic and Optical Engineering & College Microelectronics, Nanjing University of Post and Telecommunications, Nanjing 210023, P. R. China

[5]Oak Ridge National Laboratory, 1 Bethel Valley Rd, Oak Ridge, TN 37830, USA

Corresponding authors:

Anming Hu: ahu3@utk.edu

Seungha Shin : sshin@utk.edu

Author contributions:

Yongchao Yu and Yangbao Deng contributed equally to this work. Computational simulations are carried out by Md Abdullah Al Hasan.

Contents:

I. Cu Nanowire Self-Joining Phenomenon and Statistic Results

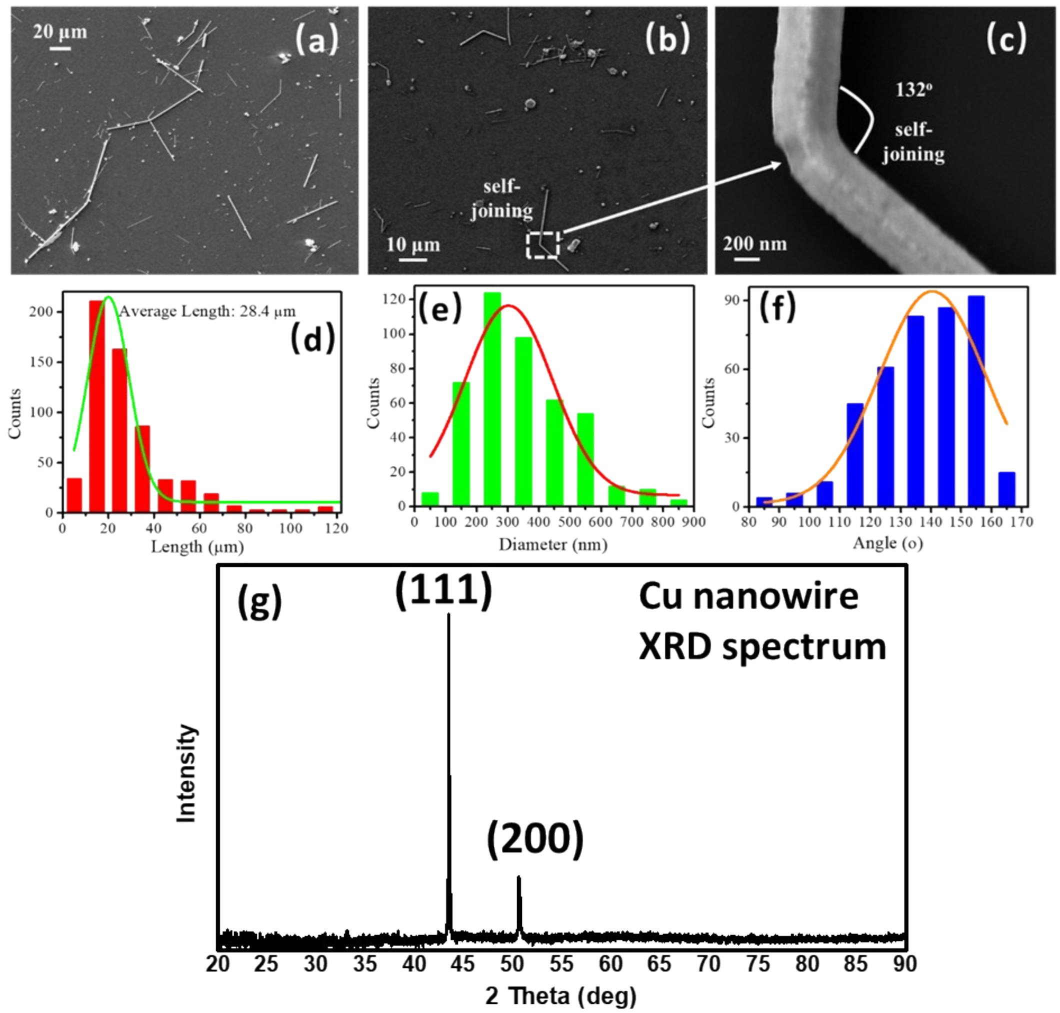

Figure S1 (a) SEM images of synthesized CuNWs, (b) SEM images of self-joined CuNWs, (c) enlarge image of self-joined CuNW for angle measurement, (d) length distribution of CuNWs, (e) diameter distribution of CuNWs, (f) angle distribution of self-joined CuNWs, and (g) XRD spectrum of synthesized CuNWs.

II. Cu Nanowire Surface Deformation after Laser Irradiation

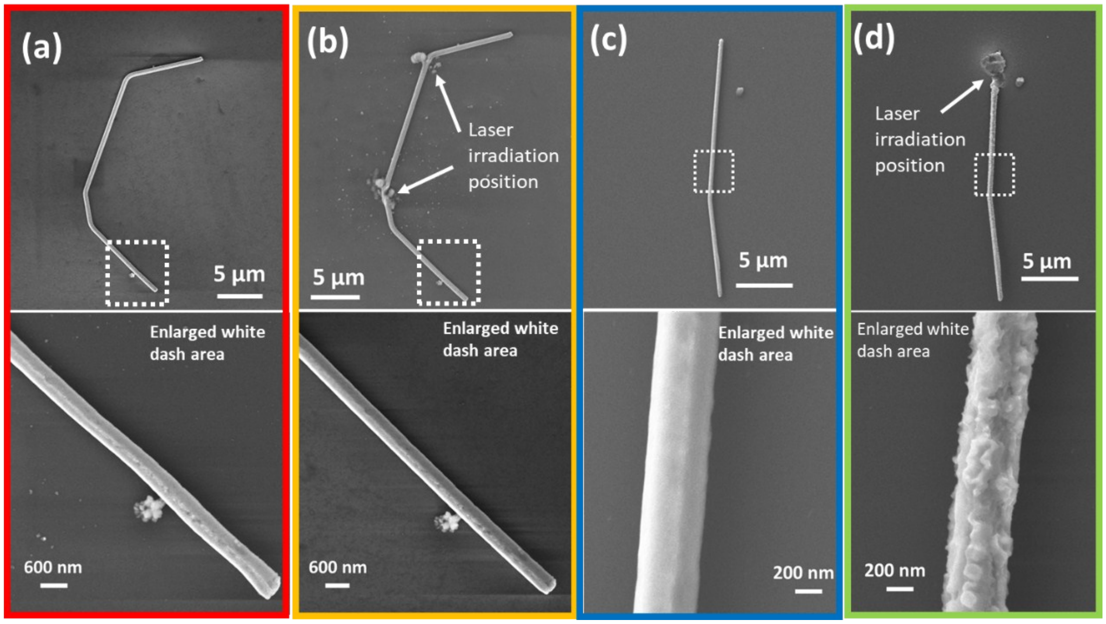

Figure S2 (a) SEM images of CuNW (a) before and (b) after FS laser irradiation, and (c) before and (d) after CW laser irradiation.

III. Comparison Between Different Laser Irradiation on CuNWs

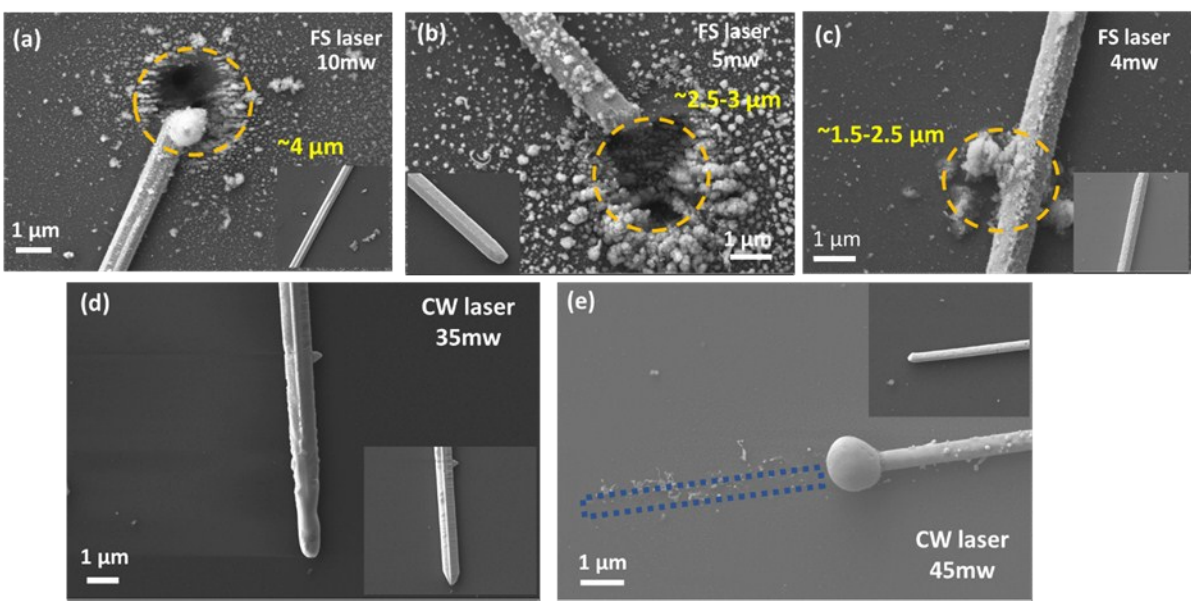

Figure S3 SEM images for FS laser irradiated nanowires with (a) 10 mW, (b) 5 mW, (c) 4 mW, and CW laser irradiated nanowires with (d) 35 mW and (e) 45 mW. Inserts show the original nanowires before laser processes.

IV. Cutting of Silver Films with a Femtosecond Pulsed Laser

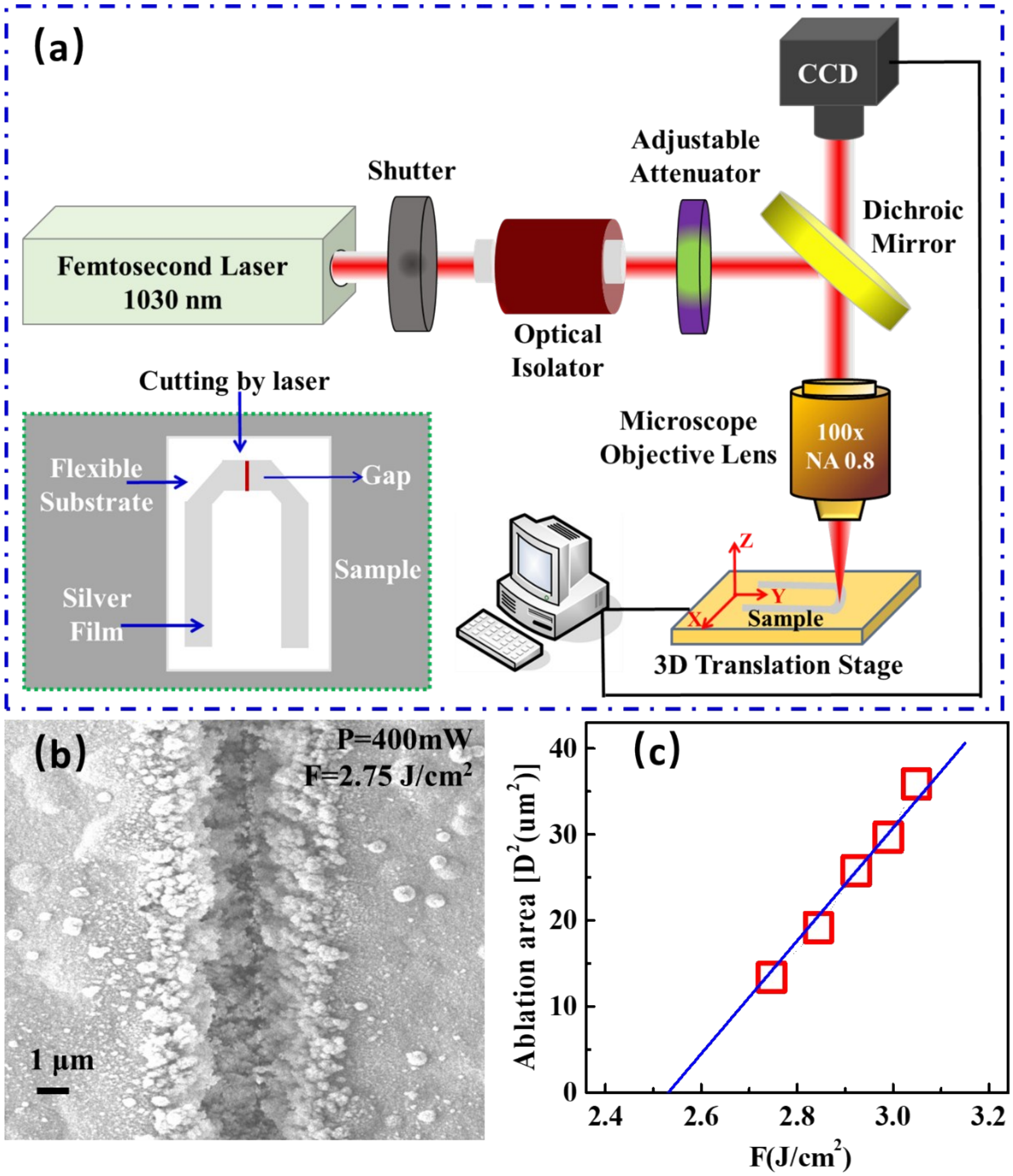

Figure S4. (a) Schematic diagram of 3D laser writing system, (b) SEM image of cutting of silver film at an incident laser fluence of 2.75 J/cm^2, (c) Liu-plot of ablation areas (D-square) as a function of incident laser fluence.

V. Manipulation of CuNWs with a Dielectrophoresis Method and Nanowire Cutting

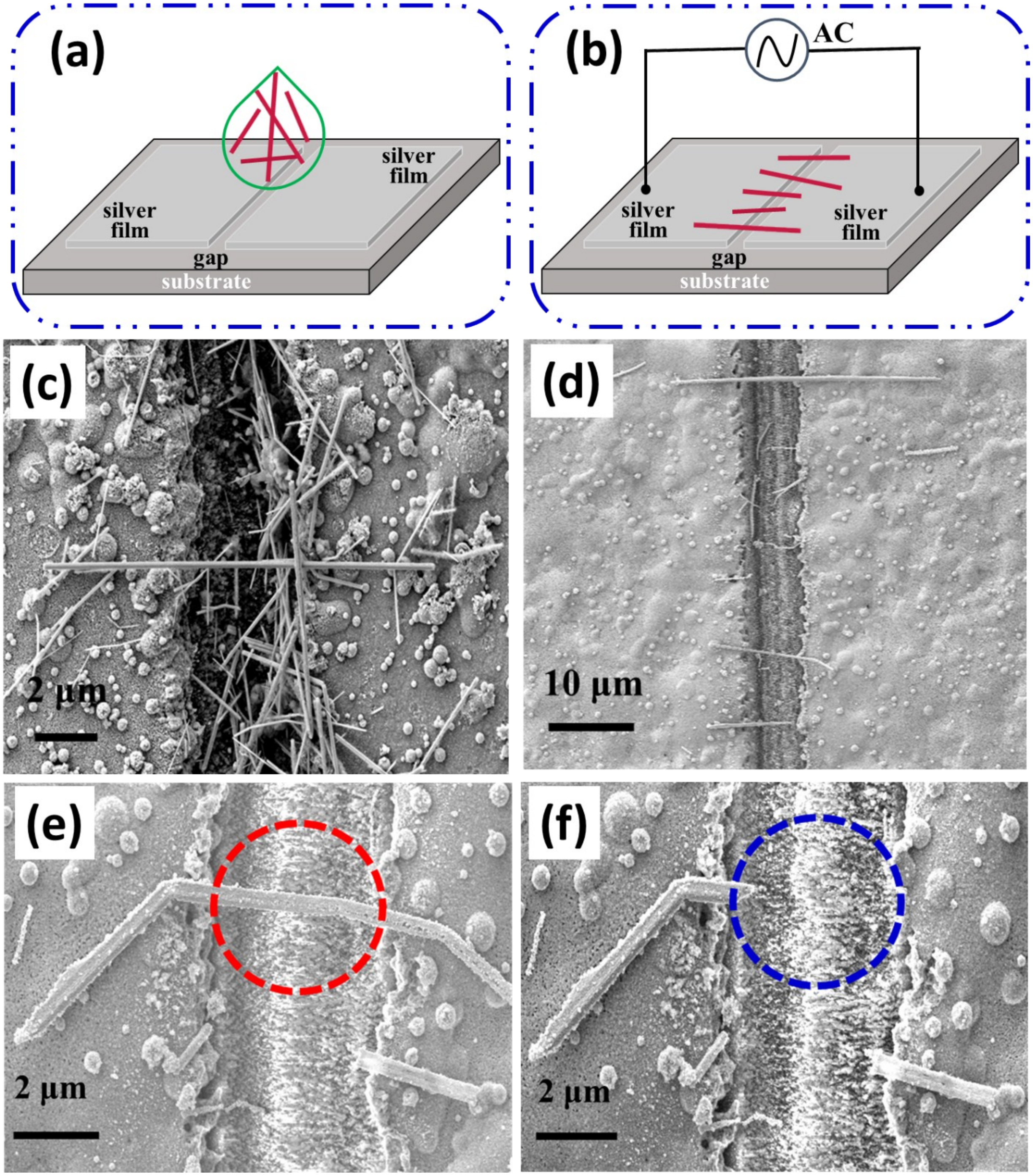

Figure S5 (a) Schematic diagram of manipulating CuNWs with a DEP method, (b) schematic of CuNWs alignment by a DEP force, (c) CuNWs bridge the gap without using AC for high concentration of CuNWs solution, (d) CuNWs bridge the gap with AC parameters of 6 V, 6 MHz, and 1 min, and (e) SEM images of CuNW before laser cutting, and (f) after laser cutting with 70 mW.

VI. Details of Computational Modeling

Simulated system:

CuNW is modeled as a cylinder with 30 μm of length and 200 nm of diameter for the thermal analysis with the1-D heat diffusion model and the finite difference method (FDM). The modeled CuNW is subdivided along the length of CuNW (i.e., in the *x* direction) as in Fig. S5. Different grid sizes are tested, and a small difference is observed in the results. Here, we select 41 equally-spaced nodal points with the distance between two nodes of 0.75 μm. The time step is set at 100 ps for the single-temperature model and 0.1 ps for the two-temperature model.

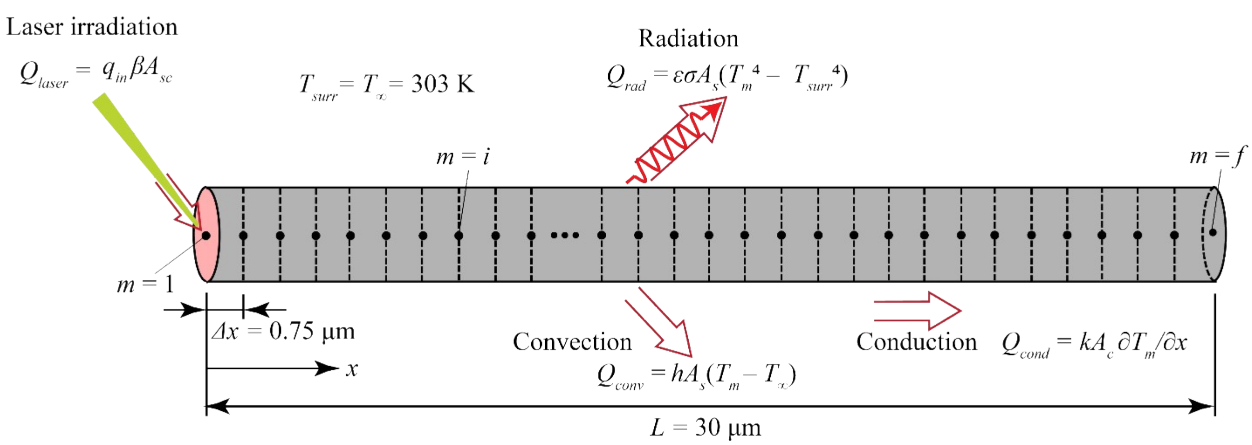

Figure S6: Computational model of 30 μm long CuNW for 1-D heat diffusion equation solved with finite difference method simulation. Convection and radiation heat transfer are considered as the experiment occurred in the ambient atmosphere. The heat source from laser is considered at the tip (first nodal point) of the CuNW.

Formulation and Discretization:

In the single-temperature model for the CW laser irradiation, the discretized heat equations for the left boundary node, inner nodes, and right boundary node are [1-3]:

$$m = 1: \quad T_1^{i+1} = 2Fo\left[\frac{A_{sc}}{A_c}\frac{q_{in}\Delta x}{k} + T_2^i + \frac{A_s}{A_c}BiT_\infty + \frac{A_s}{A_c}Bi_rT_\infty\right] + \left(1 - 2Fo - 2\frac{A_{sc}}{A_c}BiFo - 2\frac{A_{sc}}{A_c}Bi_rFo\right)T_1^i, \tag{S1.1}$$

$$1 < m < f: \quad T_m^{i+1} = Fo\left[T_{m-1}^i + T_{m+1}^i + \frac{A_s}{A_c}BiT_\infty + \frac{A_s}{A_c}Bi_rT_\infty\right] + \left(1 - 2Fo - 2\frac{A_s}{A_c}BiFo - 2\frac{A_s}{A_c}Bi_rFo\right)T_m^i, \text{and} \tag{S1.2}$$

$$m = f: \quad T_f^{i+1} = 2Fo\left[T_{f-1}^i + \frac{A_{sc}}{A_c}BiT_\infty + \frac{A_{sc}}{A_c}Bi_rT_\infty\right] + \left(1 - 2Fo - 2\frac{A_{sc}}{A_c}BiFo - 2\frac{A_{sc}}{A_c}Bi_rFo\right)T_f^i. \tag{S1.3}$$

Here, superscript i and subscript m represent the time step and nodal point, respectively (f: total number of nodal points). A_s and A_c are the side surface area of each node and cross-sectional area of the CuNW, respectively. A_{sc} indicates the surface of the boundary nodes, and q_{in} represents heat flux. Here, Fourier number, $Fo = \alpha\Delta t/\Delta x^2$, Biot number, $Bi = h\Delta x/k$, and thermal diffusivity, $\alpha = k/\rho c$. Bi_r is the radiative Biot number and is given as, $Bi_r = h_r\Delta x/k$. Here, $h_r = \varepsilon\sigma(T_m + T_{surr})(T_m^2 + T_{surr}^2)$ is the radiation heat transfer coefficient. For explicit solver, the stability condition we followed is [2],

$$Fo \cdot (1 + Bi) \leq \frac{1}{4} \tag{S2}$$

In the two-temperature model for FS laser, the discretization of the heat equation for left boundary node, inner nodes, and right boundary node is done in the following manner, respectively. At each node, the model is solved for two equations (i.e., electron temperature and lattice temperature) simultaneously.

$$m = 1: \quad \begin{aligned} T_{e,1}^{i+1} &= 2Fo\left[T_{e,2}^i + \frac{A_{sc}}{A_c}\frac{q_{in}\Delta x}{k_e}\right] + \left(1 - 2Fo_e - \frac{g\Delta t}{C_e}\right)T_{e,1}^i + \frac{g\Delta t}{C_e}T_{l,1}^i \\ T_{l,1}^{i+1} &= 2Fo\left[T_{l,2}^i + \frac{A_{sc}}{A_c}BiT_\infty + \frac{A_{sc}}{A_c}Bi_rT_\infty\right] + \left(1 - 2Fo_l - 2\frac{A_{sc}}{A_c}BiFo_l - 2\frac{A_{sc}}{A_c}Bi_rFo_l - \frac{g\Delta t}{\rho C_l}\right)T_{l,1}^i + \frac{g\Delta t}{\rho C_l}T_{e,1}^i \end{aligned} \tag{S3.1}$$

$1 < m < f$:

$$T_{e,k}^{i+1} = Fo\left[T_{e,k-1}^{i} + T_{e,k+1}^{i}\right] + \left(1 - 2Fo_e - \frac{g\Delta t}{C_e}\right)T_{e,k}^{i} + \frac{g\Delta t}{C_e}T_{l,k}^{i}$$

$$T_{l,k}^{i+1} = Fo\left[T_{l,k-1}^{i} + T_{l,k+1}^{i} + \frac{A_s}{A_c}BiT_\infty + \frac{A_s}{A_c}Bi_r T_\infty\right] + \left(1 - 2Fo_l - \frac{A_s}{A_c}BiFo_l - \frac{A_s}{A_c}Bi_r Fo_l - \frac{g\Delta t}{\rho C_l}\right)T_{l,k}^{i} + \frac{g\Delta t}{\rho C_l}T_{e,k}^{i} \quad \text{(S3.2)}$$

$m = f$:

$$T_{e,f}^{i+1} = 2Fo\left[T_{e,f-1}^{i}\right] + \left(1 - 2Fo - \frac{g\Delta t}{C_e}\right)T_{e,f}^{i} + \frac{g\Delta t}{C_e}T_{l,f}^{i}$$

$$T_{l,f}^{i+1} = 2Fo\left[T_{l,f-1}^{i} + \frac{A_{sc}}{A_c}BiT_\infty + \frac{A_{sc}}{A_c}Bi_r T_\infty\right] + \left(1 - 2Fo - 2\frac{A_{sc}}{A_c}BiFo_l - 2\frac{A_{sc}}{A_c}Bi_r Fo - \frac{g\Delta t}{\rho C_l}\right)T_{l,f}^{i} + \frac{g\Delta t}{\rho C_l}T_{e,f}^{i}$$

(S3.3)

Power Calculation:

For CW laser, we calculated heat flux from the following equation,

$$q_{in} = \frac{\text{Power}}{\text{Heated area}} = \frac{P}{\pi d_{LB}^2/4}, \quad \text{(S4)}$$

where CW laser power, P = 35 mW and laser beam diameter (d_{LB}) is considered as 1 μm. The measured heat flux of 4.46×10^6 W/cm^2 is used in our simulations.

For FS laser:

$$\text{Energy per pulse} = \frac{\text{Average power}}{\text{Pulse frequency}}$$

$$\text{Peak power} = \frac{\text{Energy per pulse}}{\text{Pulse length}}, \quad \text{(S5)}$$

where the FS laser pulse frequency is 120 kHz, the pulse length is 300 fs, and two different average power, i.e., 5 mW and 35 mW, are employed. Then, using the peak power from Eq. (S5) for Eq. (S4), the heat flux during each FS laser pulse is calculated as 1.77×10^{13} W/cm^2 for average power of 5 mW and 1.24×10^{14} W/cm^2 for 35 mW. Several heat convection coefficients are tested, and the resulting temperature distribution does not vary significantly. Here, we select heat convection coefficient, h = 2,000 W/m^2-K for further study.

References

[1] J. H. Lienhard, "A heat transfer textbook" (Courier Corporation, 2011)

[2] F. P. Incropera, A. S. Lavine, T. L. Bergman, and D. P. DeWitt, "Fundamentals of heat and mass transfer" (Wiley, 2007)

[3] Y. A. Cengel, "Heat Transfer" (McGraw-Hill, 2007).

1. J. H. Lienhard, *A heat transfer textbook*, Courier Corporation, 2011.
2. F. P. Incropera, A. S. Lavine, T. L. Bergman and D. P. DeWitt, *Fundamentals of heat and mass transfer*, Wiley, 2007.
3. A. Cengel, 2007.